Supplement of Aerosol Research, 2, 271–289, 2024
https://doi.org/10.5194/ar-2-271-2024-supplement

AEROSOL Research
Open Access

Supplement of

Comparison of size distribution and electrical particle sensor measurement methods for particle lung deposited surface area ($LDSA^{al}$) in ambient measurements with varying conditions

Teemu Lepistö et al.

Correspondence to: Teemu Lepistö (teemu.lepisto@tuni.fi)

Measurement locations

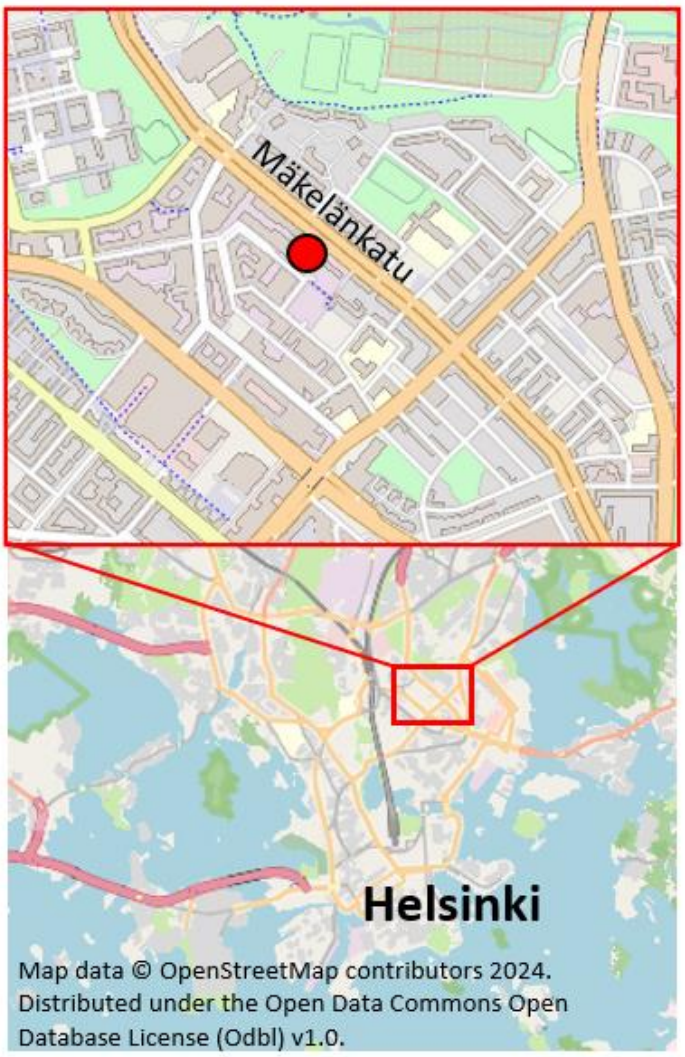

Figure S1: Measurement location in Helsinki (see also Teinilä et al. 2024)

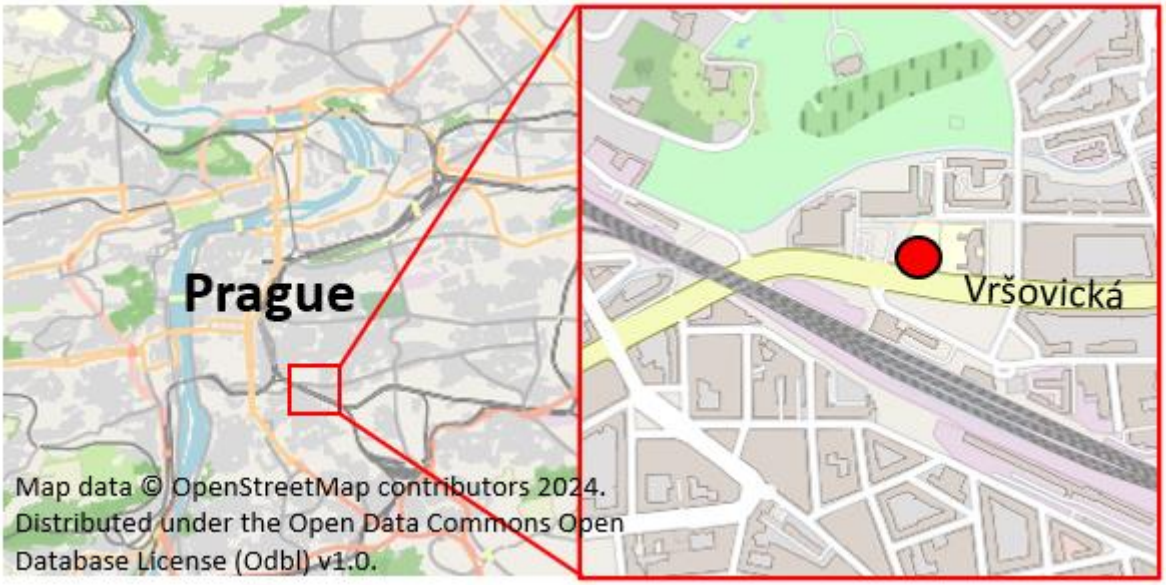

Figure S2: Measurement location in Prague (see also Lepistö et al. 2023)

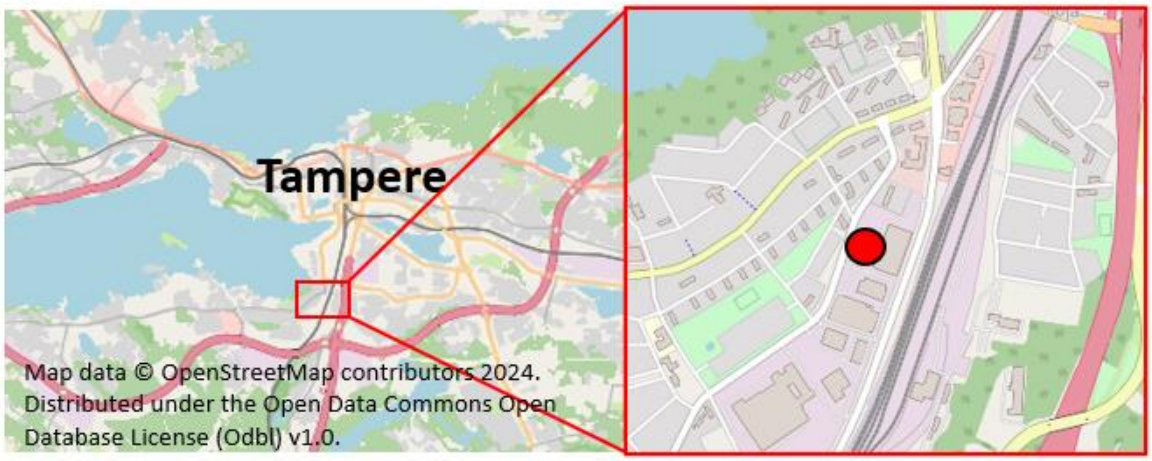

Figure S3: Measurement location in Tampere (see also Silvonen et al. 2023)

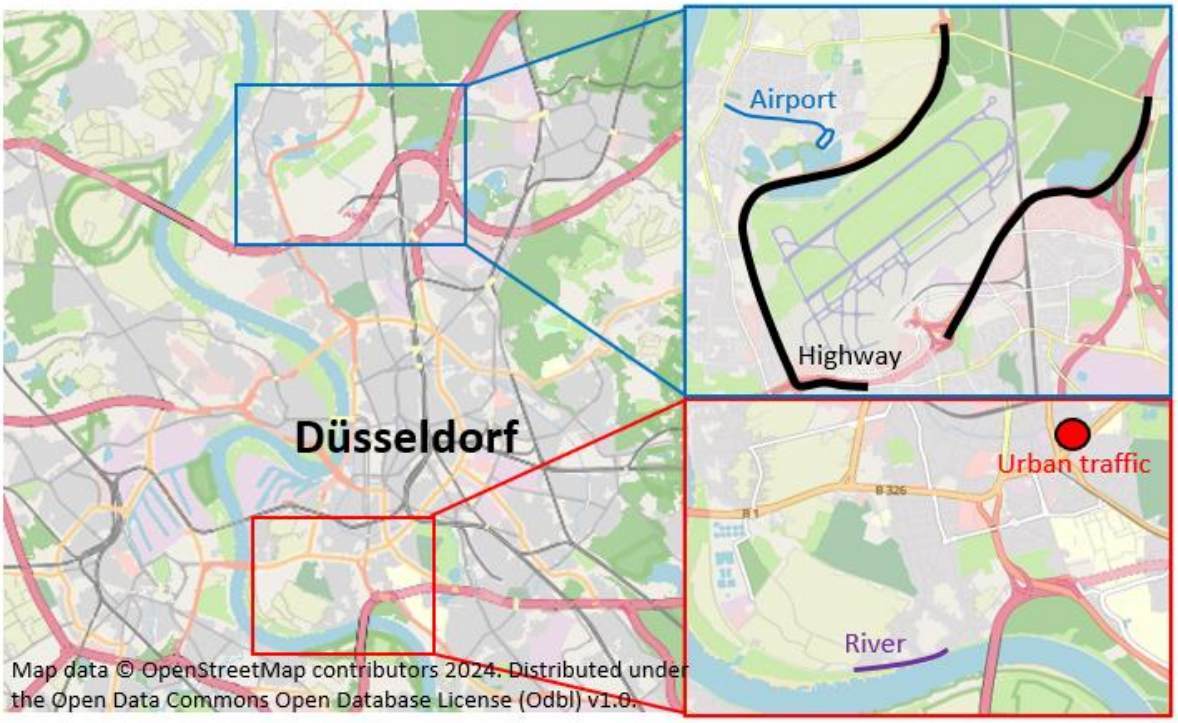

Figure S4: Measurement locations in Düsseldorf. Black and purple lines indicate driving measurements, and the red dot stationary measurements (see also Lepistö et al. 2023)

Table S1: Parameters utilised in the ICRP model calculation (ICRP 1994, Hinds 1999)

	Functional Reserve Capacity, FRC (l)	**Breathing rate (m^3/h)**	**Breathing Frequency (1/min)**	**Tidal Volume (l)**
Female				
Sitting	*2.68*	*0.39*	*14*	*0.46*
Light Exercise	*2.68*	*1.25*	*21*	*0.99*
Heavy Exercise	*2.68*	*2.7*	*33*	*1.36*
Male				
Sitting	*3.30*	*0.54*	*12*	*0.75*
Light Exercise	*3.30*	*1.5*	*20*	*1.25*
Heavy Exercise	*3.30*	*3*	*26*	*1.92*

Particle effective density

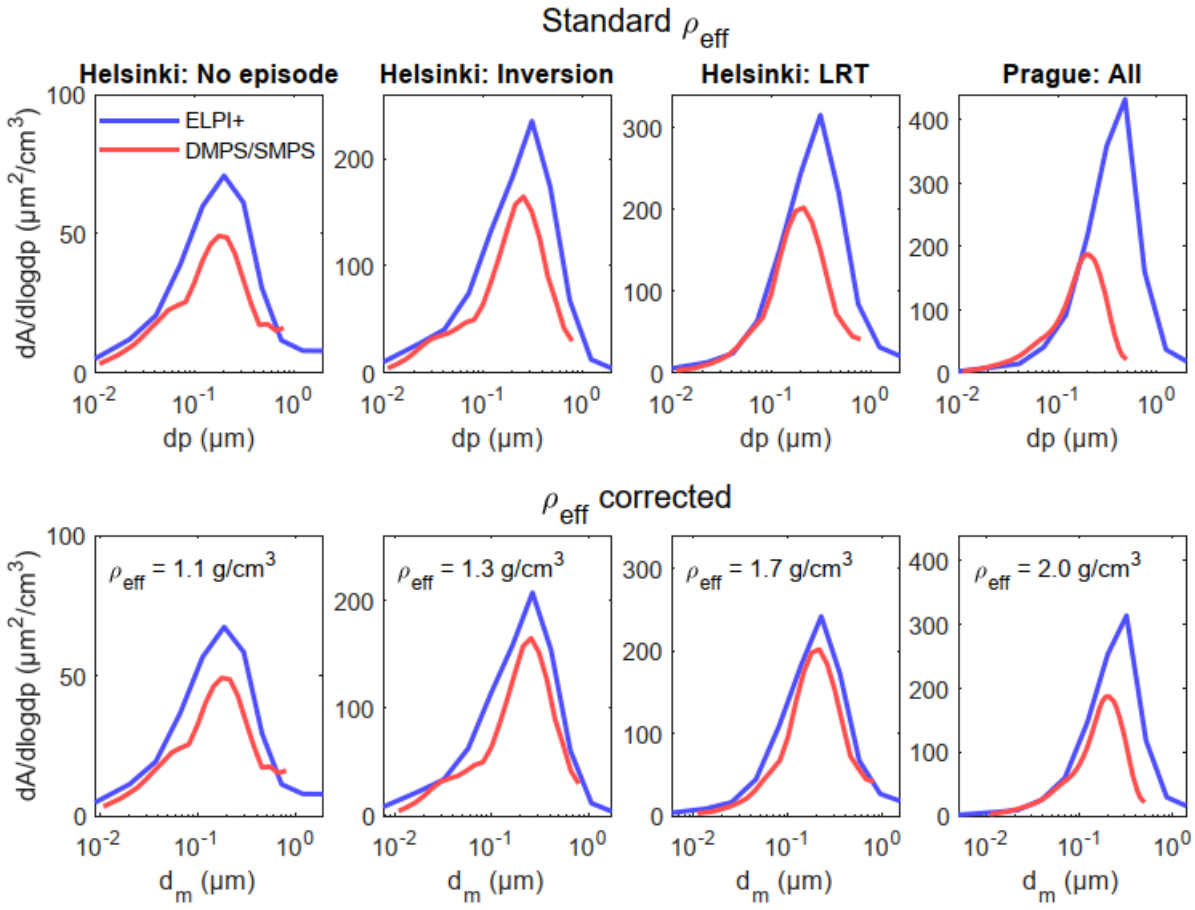

Figure S5: Average particle surface area size distributions measured with the ELPI+, DMPS (Helsinki) and SMPS (Prague) during the studied periods with and without corrections for the particle effective density.

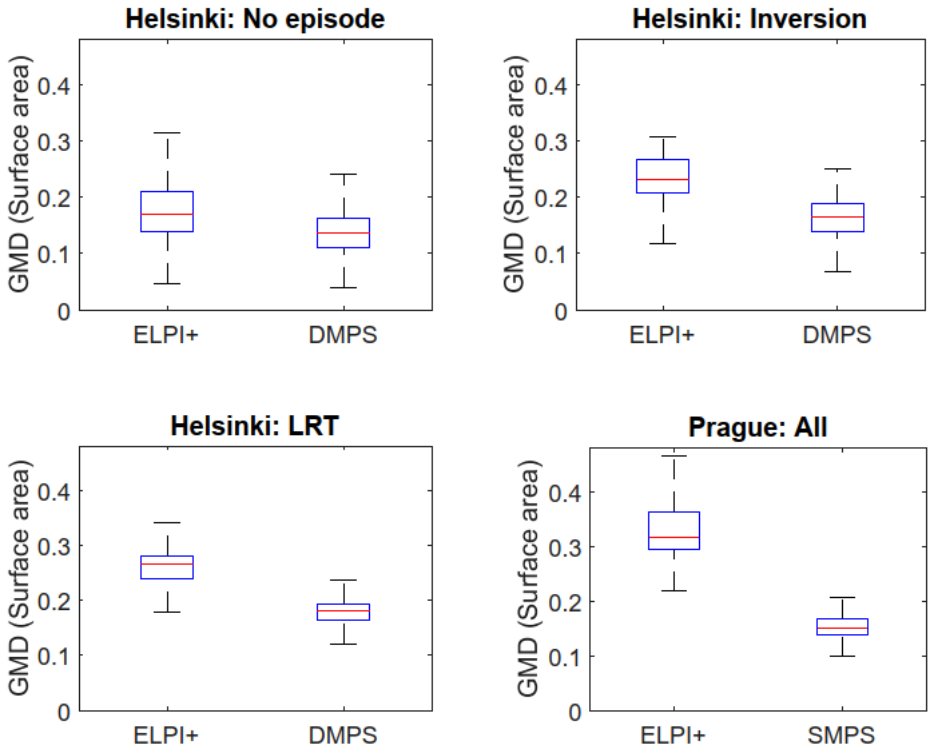

Figure S6: Boxplots of the measured geometric mean diameters of particle surface area size distributions with the ELPI+ (aerodynamic diameter) and DMPS or SMPS (mobility equivalent diameter).

Particle hygroscopicity and the lung deposition

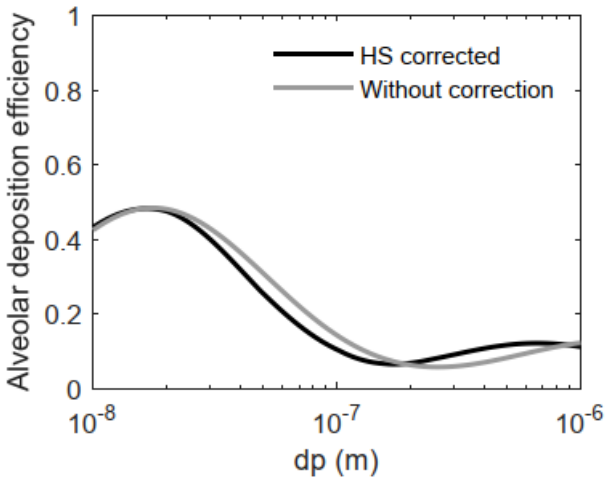

Figure S7: The utilised function of particle lung deposition efficiency (standard ρ_{eff}) in the lung alveoli with and without correction for the particle hygroscopicity (Vu et al. 2015) for road traffic environments.

Histograms of the measured concentrations

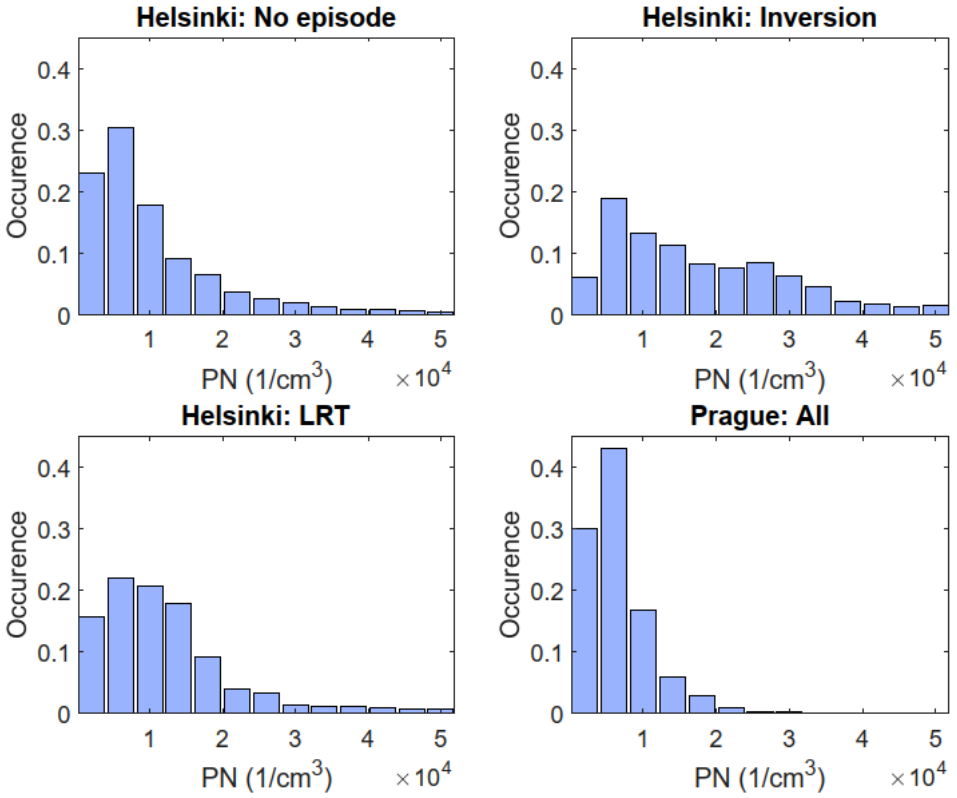

Figure S8: Histogram of the measured particle number (PN) concentrations in Helsinki and Prague.

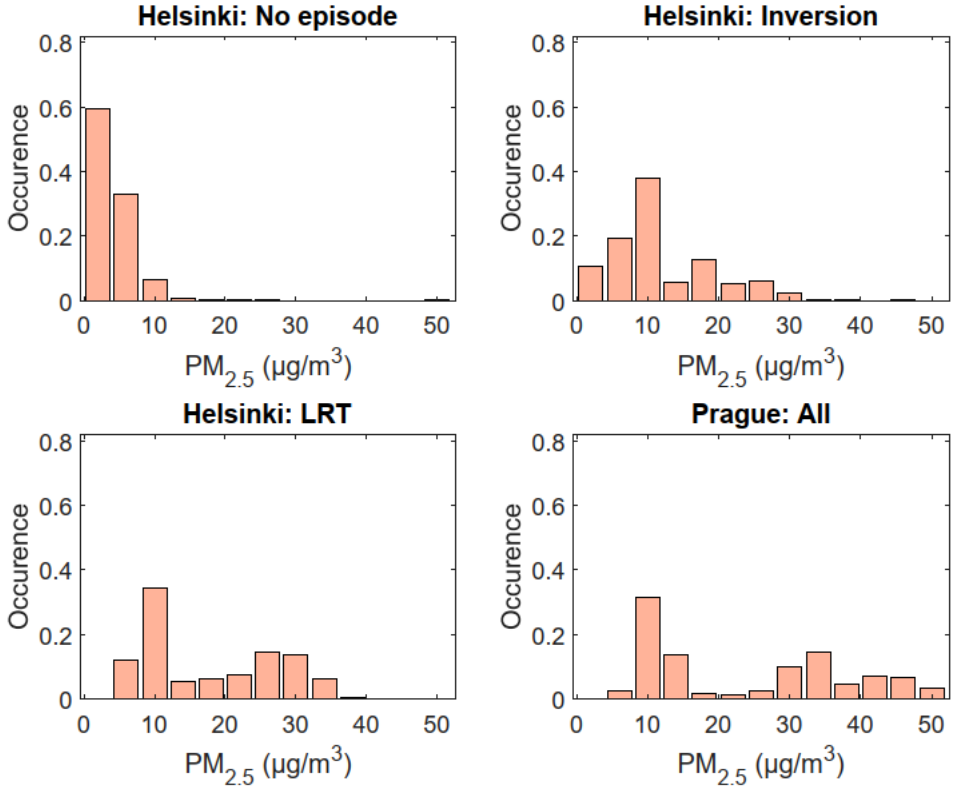

Figure S9: Histogram of the measured $PM_{2.5}$ concentrations in Helsinki and Prague measurements.

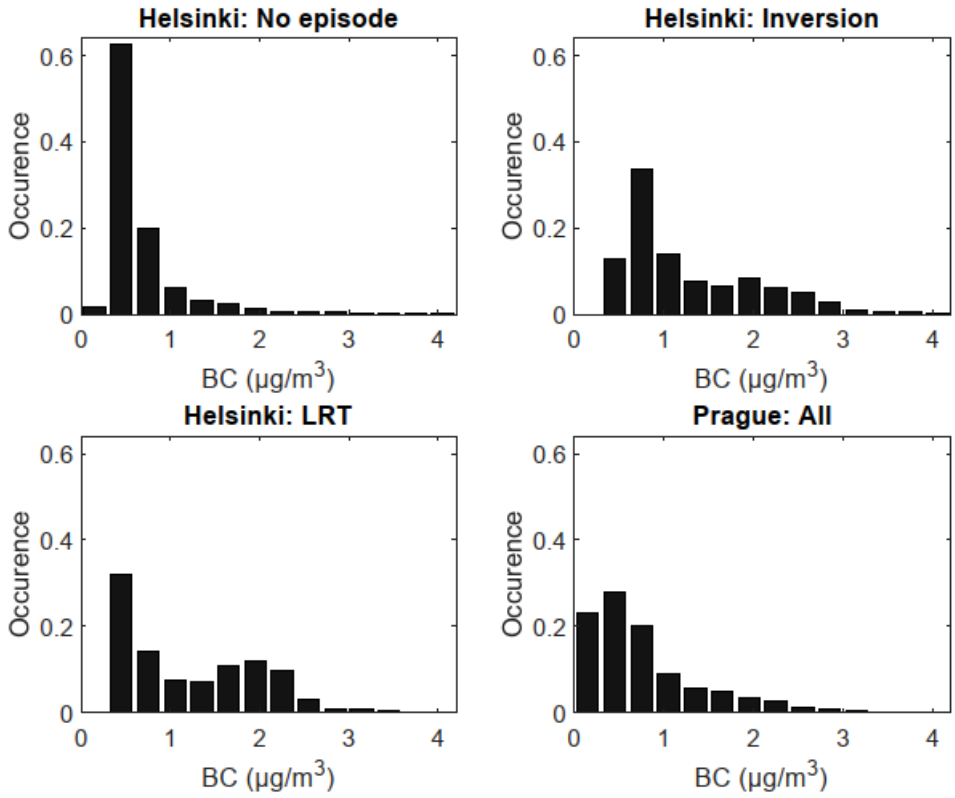

Figure S10: Histogram of the measured black carbon (BC) concentrations in Helsinki and Prague measurements.

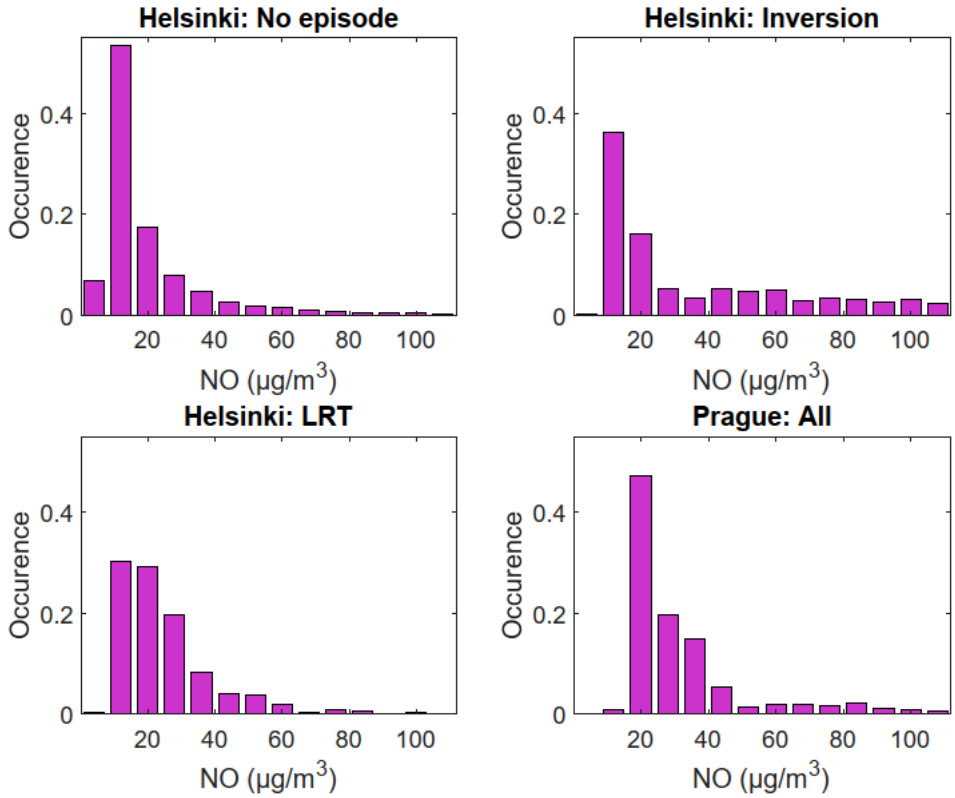

Figure S11: Histogram of the measured NO concentrations in Helsinki and Prague measurements.

LDSA^{al} concentrations

Table S2: Data of the measured average LDSA^{al} concentrations in Figures 1–6, including the 25th and 75th percentile whiskers. Note that Partector results cannot be corrected based on the particle effective density (ρ_{eff}) nor hygroscopicity.

Helsinki: No episodes, LDSA^{al} (µm^2/cm^3)

	ELPI+	DMPS	Partector
General assumptions	*11.5 (6.9–17.7)*	*8.5 (5.0–13.7)*	10.5 (6.1–17.0)
ρ_{eff}-corrected	*11.3 (6.8–17.4)*	*8.6 (5.0–13.8)*	
ρ_{eff}- and hygroscopicity corrected	*10.2 (6.2–15.7)*	*8.2 (4.9–12.8)*	

Helsinki: Inversion, LDSA^{al} (µm^2/cm^3)

	ELPI+	DMPS	Partector
General assumptions	*28.4 (16.3–53.9)*	*20.2 (11.1–39.3)*	24.7 (13.1–45.8)
ρ_{eff}-corrected	*26.7 (15.3–51.9)*	*20.5 (11.2–39.9)*	
ρ_{eff}- and hygroscopicity corrected	*26.5 (16.1–49.4)*	*20.7 (12.0–38.6)*	

Helsinki: LRT, LDSA^{al} (µm^2/cm^3)

	ELPI+	DMPS	Partector
General assumptions	*26.9 (15.6–46.6)*	*18.6 (11.0–30.9)*	20.5 (11.5–34.1)
ρ_{eff}-corrected	*24.7 (14.5–42.7)*	*19.5 (11.4–32.7)*	
ρ_{eff}- and hygroscopicity corrected	*23.6 (12.8–44.8)*	*19.6 (11.0–34.4)*	

Prague: All, LDSA^{al} (µm^2/cm^3)

	ELPI+	SMPS	Partector
General assumptions	*27.1 (15.6–42.3)*	*14.7 (9.5–20.5)*	18.1 (11.6–25.0)
ρ_{eff}-corrected	*23.3 (13.6–35.7)*	*15.5 (9.9–21.7)*	
ρ_{eff}- and hygroscopicity corrected	*24.7 (14.8–38.0)*	*15.0 (9.4–21.1)*	

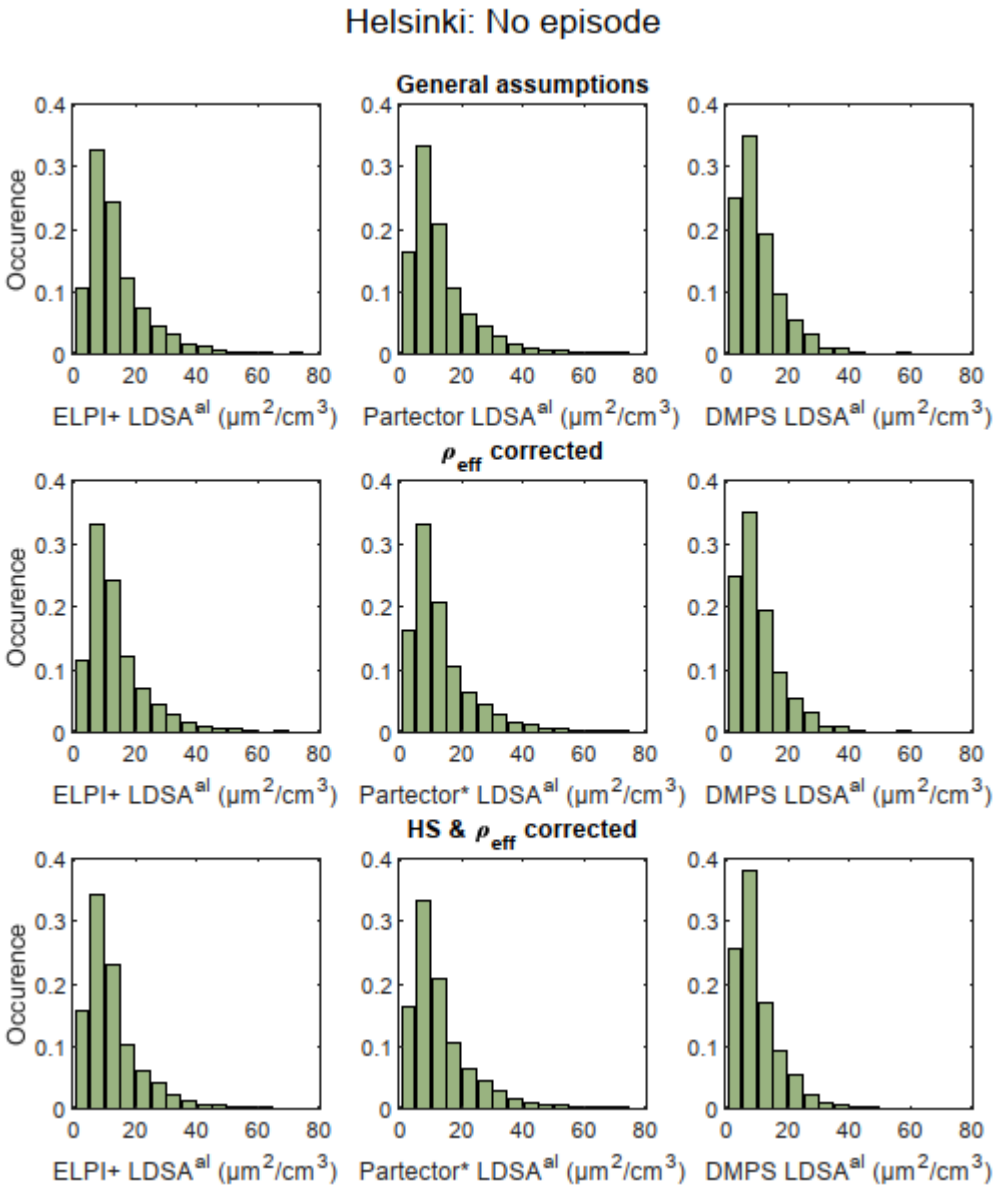

Figure S12: Histograms of the measured $LDSA^{al}$ concentrations with general assumptions, with effective density (ρ_{eff}) correction, and with corrections for hygroscopicity (HS) and effective density in Helsinki without episodes. *Note that effective density and hygroscopicity cannot be considered in the Partector results.

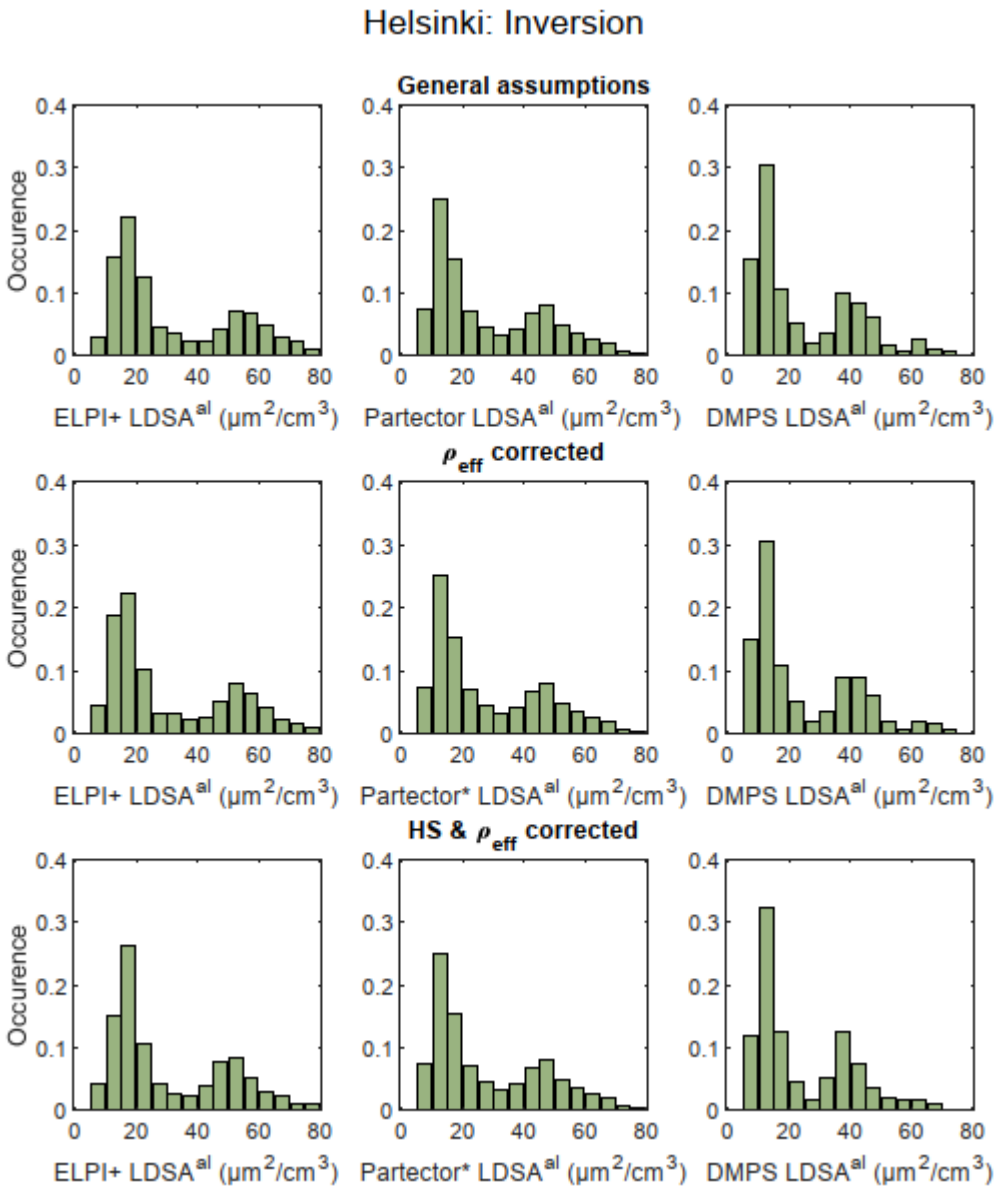

Figure S13: Histograms of the measured $LDSA^{al}$ concentrations with general assumptions, with effective density (ρ_{eff}) correction, and with corrections for hygroscopicity (HS) and effective density in Helsinki during the inversion episode. *Note that effective density and hygroscopicity cannot be considered in the Partector results.

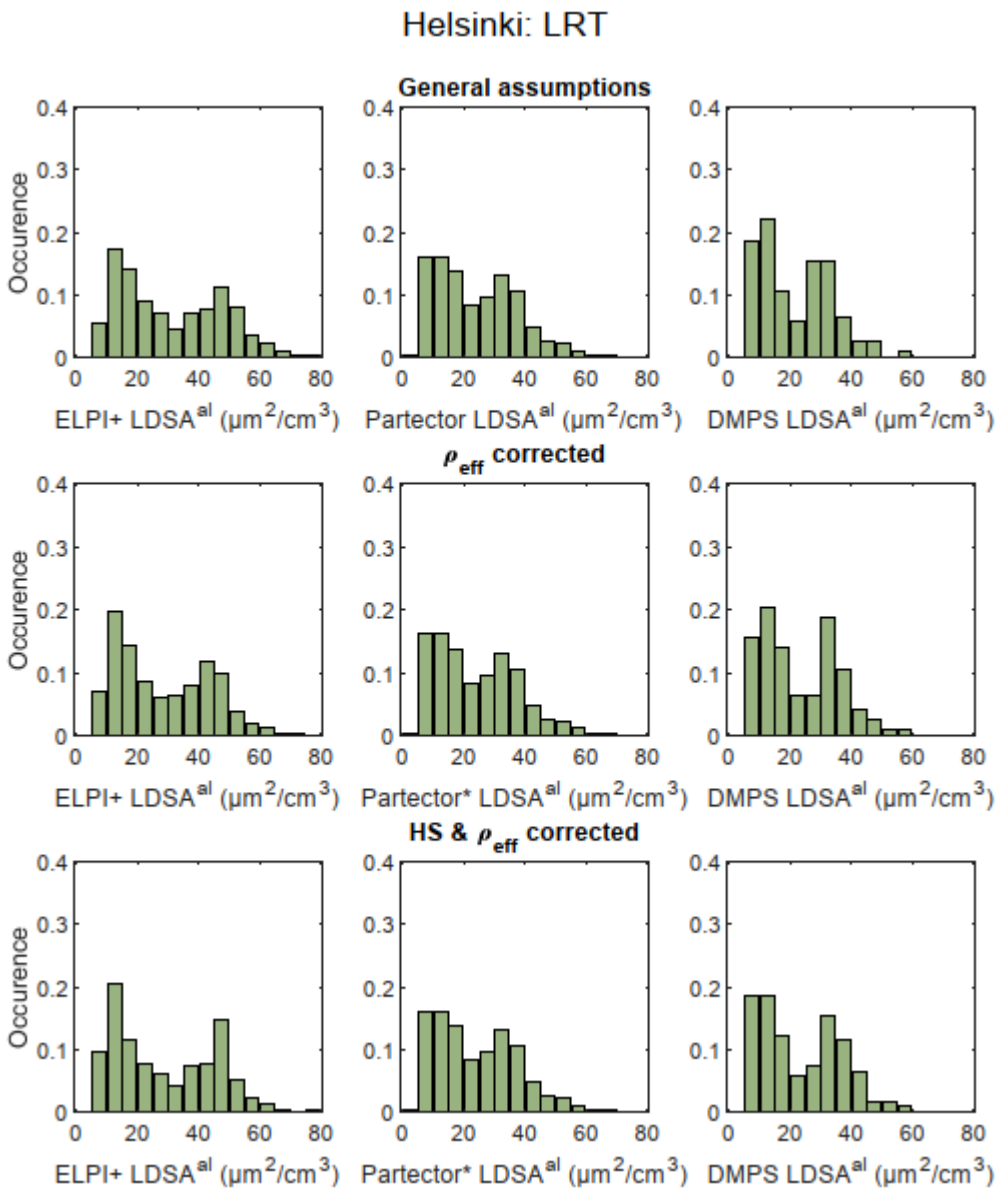

Figure S14: Histograms of the measured LDSA^{al} concentrations with general assumptions, with effective density (ρ_{eff}) correction, and with corrections for hygroscopicity (HS) and effective density in Helsinki during the LRT episode. *Note that effective density and hygroscopicity cannot be considered in the Partector results.

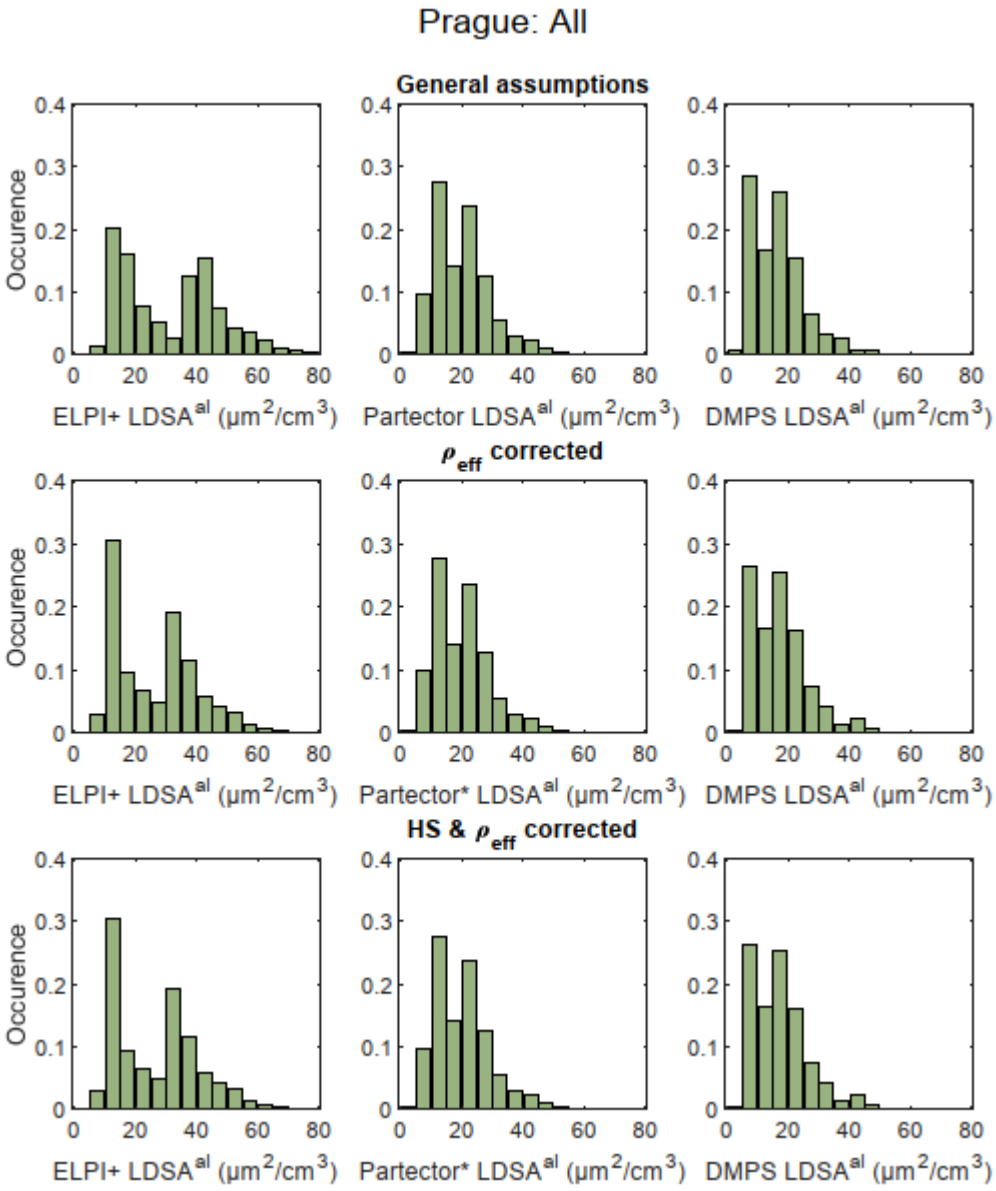

Figure S15: Histograms of the measured $LDSA^{al}$ concentrations with general assumptions, with effective density (ρ_{eff}) correction, and with corrections for hygroscopicity (HS) and effective density in Prague. *Note that effective density and hygroscopicity cannot be considered in the Partector results.

Table S3: Average measured concentrations, including 25th and 75th percentiles in Figure 8 and Figure S20-22.

	ELPI+ LDSA^{al} < 2.5 µm (µm^2/cm^3)	**ELPI+ LDSA^{al} < 0.4 µm (µm^2/cm^3)**	**Partector LDSA^{al} (µm^2/cm^3)**	**ELPI+ PN (1/cm^3)**	**ELPI+ $PM_{2.5}$ (µg/m^3)**
Helsinki: No episode	*11.5 (6.9–17.7)*	*9.8 (5.7–16.0)*	*10.5 (6.1–17.0)*	*7 700 (4 100–13 700)*	*3.4 (2.3–5.2)*
Helsinki: Inversion	*28.4 (16.3–53.9)*	*22.9 (11.9–45.3)*	*24.7 (13.1–45.8)*	*16 200 (8 100–29 200)*	*9.9 (7.2–16.6)*
Helsinki: LRT	*26.9 (15.6–46.6)*	*19.1 (11.1–31.2)*	*20.5 (11.5–34.1)*	*9 700 (5 600–15 500)*	*15.4 (9.5–26.8)*
Prague: All	*27.1 (15.6–42.3)*	*14.0 (9.2–19.4)*	*18.1 (11.6–25.0)*	*5 700 (3 700–8 100)*	*20.2 (11.1–35.3)*
Tampere: No episode	*8.3 (4.7–13.9)*	*5.7 (3.2–9.6)*	*6.3 (3.6–10.3)*	*2 800 (1 400–5 900)*	*4.2 (2.4–8.2)*
Tampere: Inversion	*55.5 (40.6–86.9)*	*44.6 (31.4–68.9)*	*46.8 (33.9–71.9)*	*23 800 (16 700–34 500)*	*22.9 (16.2–38.0)*
Düsseldorf: Urban traffic	*31.8 (21.3–49.3)*	*18.8 (13.4–23.4)*	*21.0 (15.1–26.7)*	*12 700 (8 700–16 600)*	*20.7 (12.0–35.1)*
Düsseldorf: Highway	*36.6 (24.8–47.5)*	*27.2 (17.9–38.3)*	*30.8 (20.6–43.5)*	*28 900 (16 300–48 700)*	*17.1 (11.6–24.6)*
Düsseldorf: Airport	*34.2 (30.6–41.9)*	*24.4 (19.1–31.7)*	*27.4 (21.8–35.6)*	*26 400 (16 100–44 500)*	*16.9 (13.0–25.5)*
Düsseldorf: River	*33.0 (24.9–50.2)*	*17.6 (12.5–24.9)*	*20.8 (15.2–28.5)*	*11 700 (8 300–13 600)*	*24.6 (19.7–44.3)*

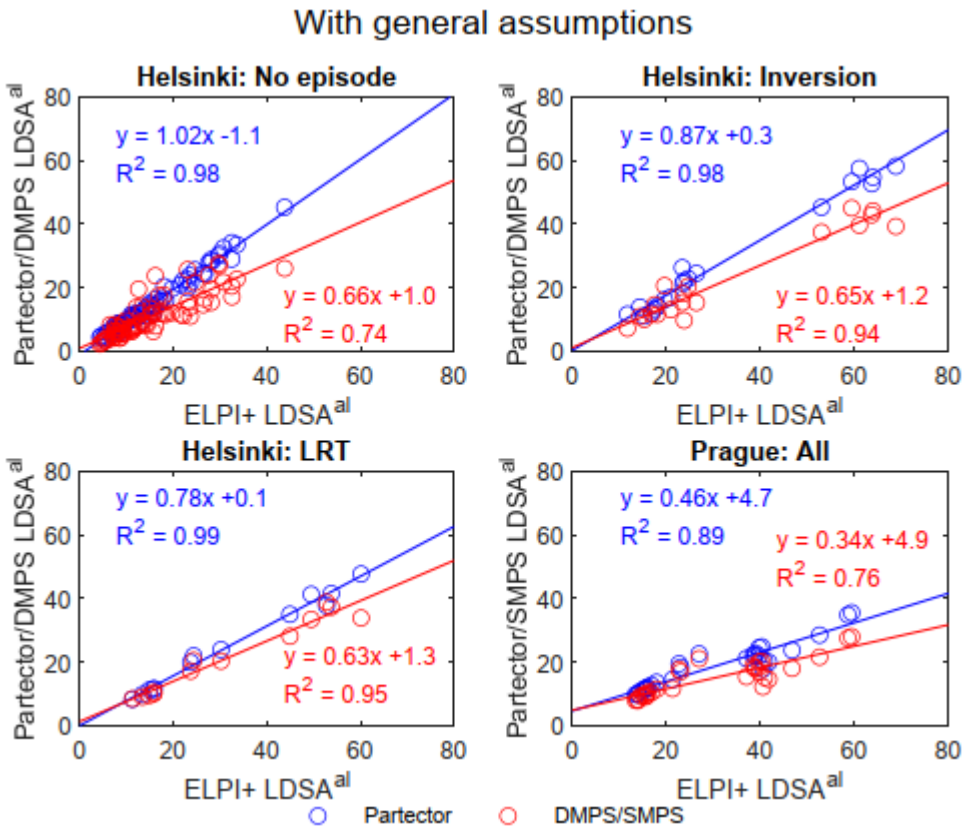

Figure S16: Scatter plot and linear fits between hourly averaged ELPI+ LDSA^{al} (µm^2/cm^3) and Partector or DMPS/SMPS LDSA^{al} (µm^2/cm^3) with general assumptions.

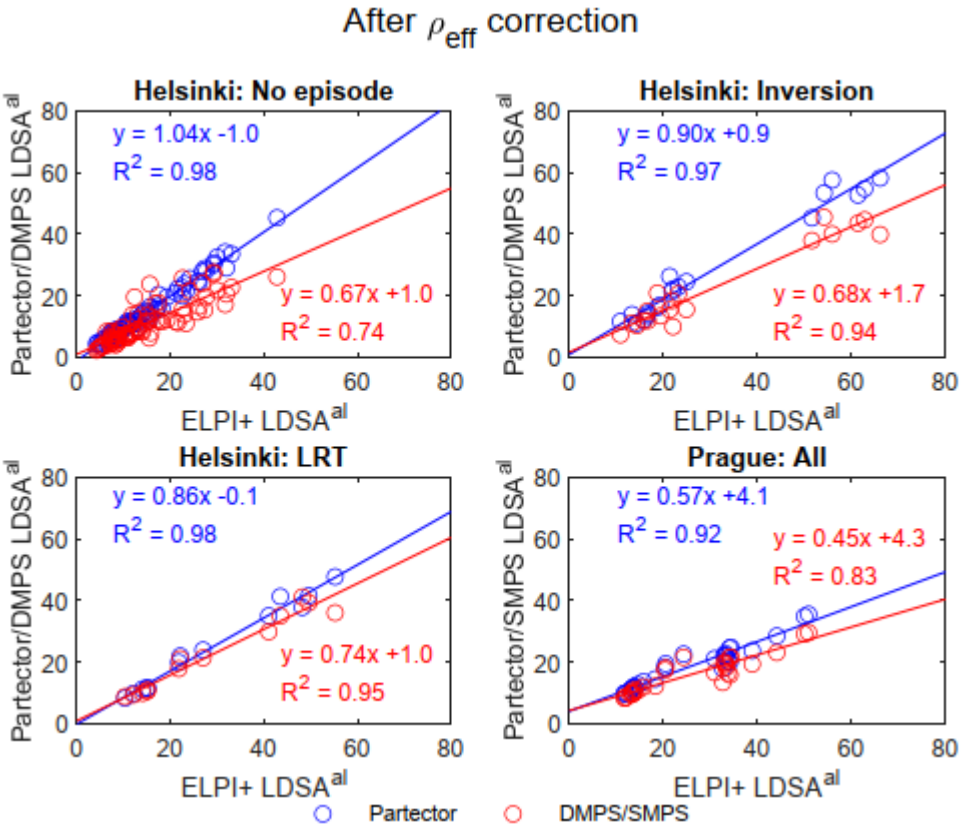

Figure S17: Scatter plot and linear fits between hourly averaged ELPI+ LDSA^{al} (µm^2/cm^3) and Partector or DMPS/SMPS LDSA^{al} (µm^2/cm^3) after ρ_{eff} correction (not for Partector).

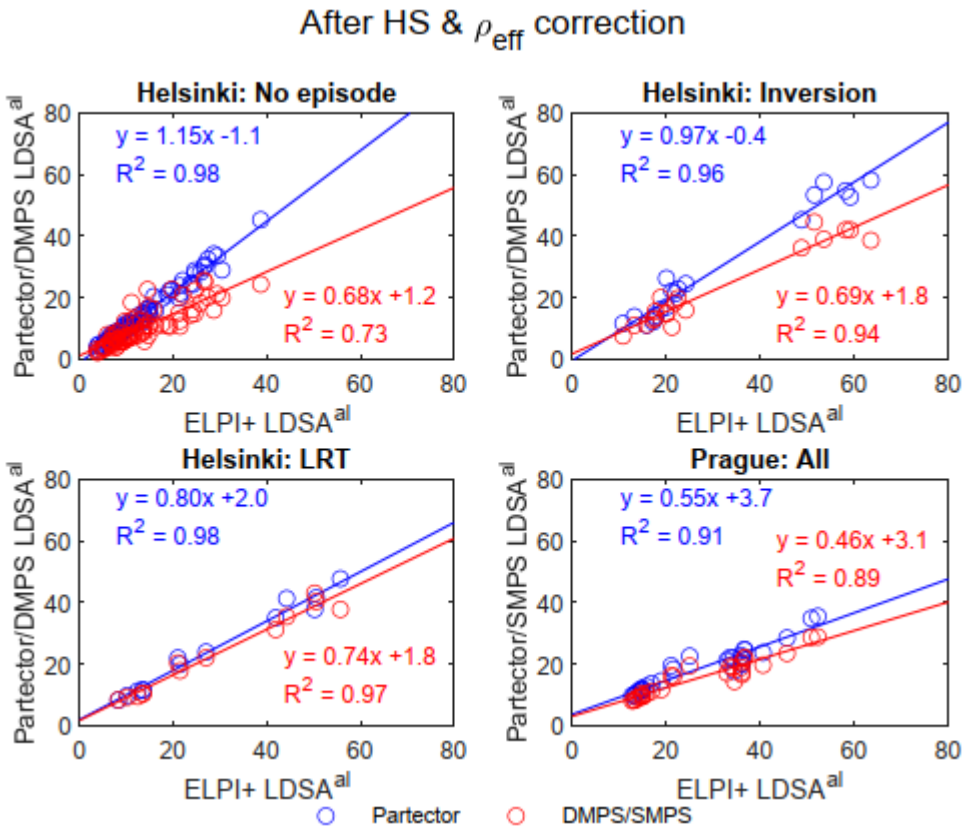

Figure S18: Scatter plot and linear fits between hourly averaged ELPI+ LDSA^{al} (µm^2/cm^3) and Partector or DMPS/SMPS LDSA^{al} (µm^2/cm^3) after hygroscopicity (HS) and ρ_{eff} correction (not for Partector).

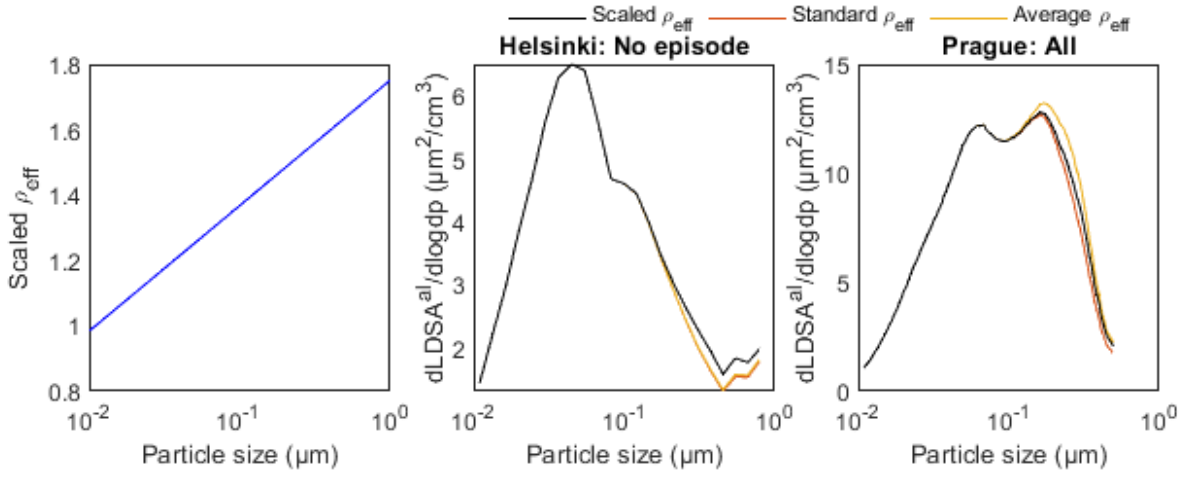

Figure S19: Comparison of average LDSA^{al} size distributions with Helsinki: All (DMPS) and Prague: All (SMPS) data by using scaled size-dependent effective density (ρ_{eff}), standard ρ_{eff} (1.0 g/cm^3) and averaged ρ_{eff} for all sizes (Helsinki: 1.1 g/cm^3, Prague 2.0 g/cm^3). Scaled ρ_{eff} function is showed in the first figure panel and is based on studies by Virtanen et al. (2006), Rissler et al. (2014), Yin et al. (2015) and Lu et al. (2024).

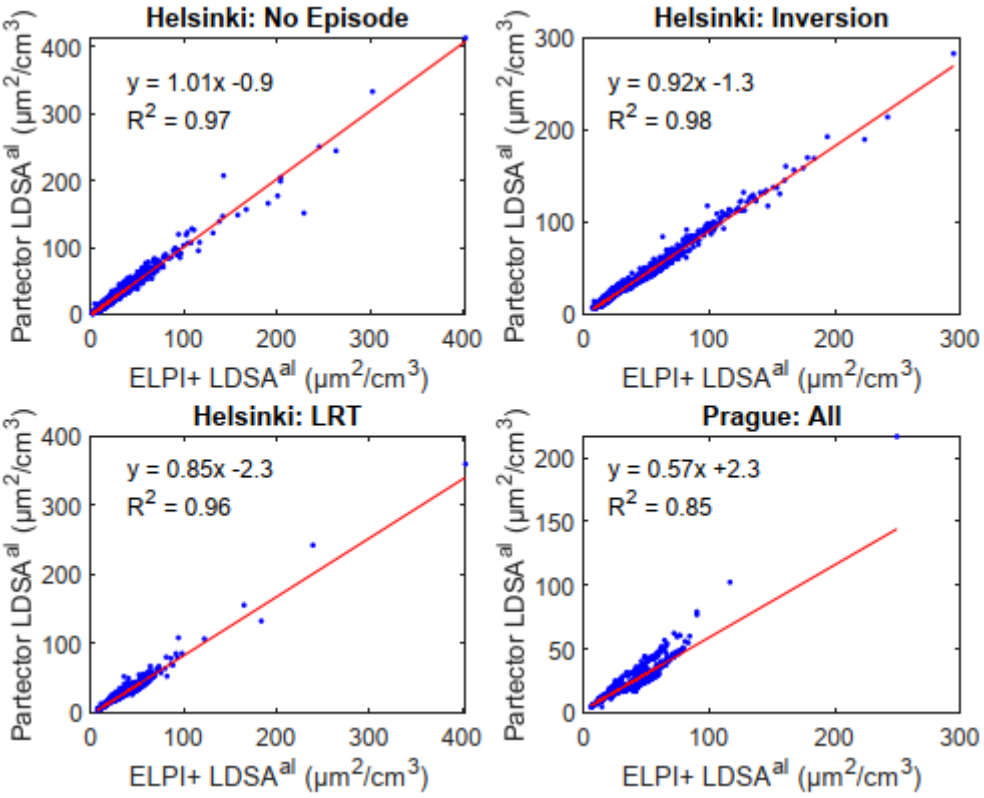

Figure S20: Scatter plots between measured $LDSA^{al}$ concentrations with the ELPI+ and the Partector (with general assumptions) in Helsinki and Prague. Outliers of $LDSA^{al} > 500$ µm²/cm³ were removed from the scatter plots.

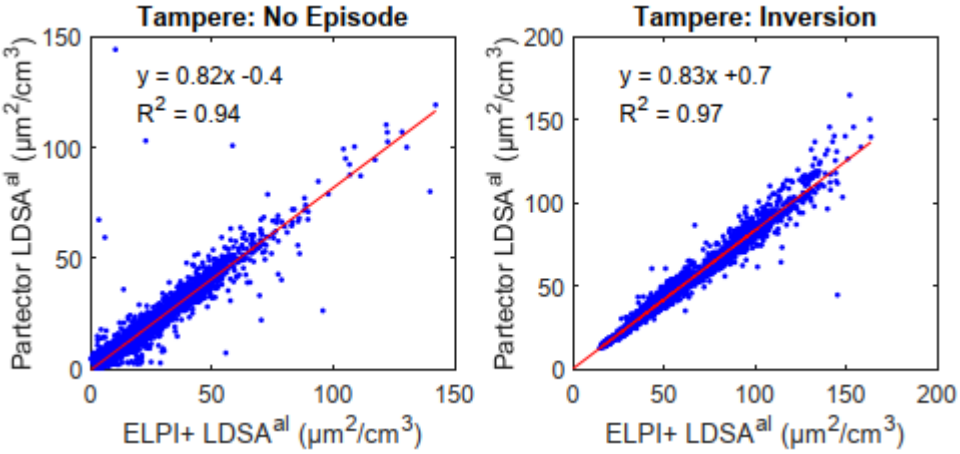

Figure S21: Scatter plots between measured $LDSA^{al}$ concentrations with the ELPI+ and the Partector (with general assumptions) in Tampere. Outliers of $LDSA^{al} > 500$ µm²/cm³ were removed from the scatter plots.

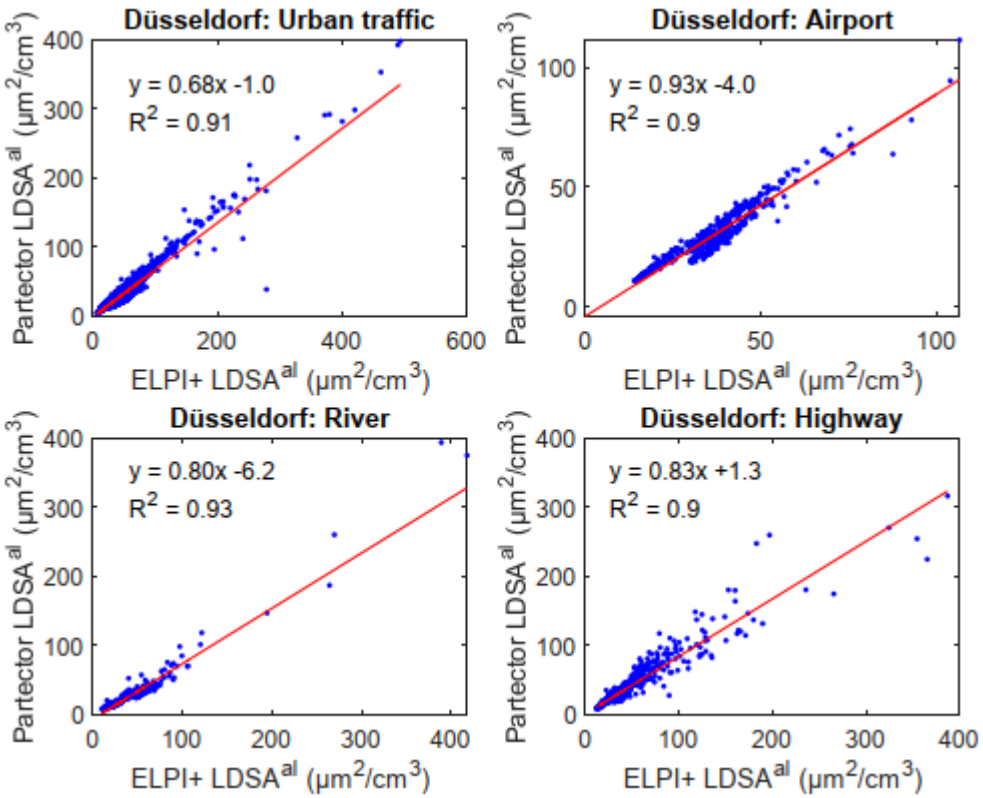

Figure S22: Scatter plots between measured $LDSA^{al}$ concentrations with the ELPI+ and the Partector (with general assumptions) in Düsseldorf. Outliers of $LDSA^{al} > 500$ µm²/cm³ were removed from the scatter plots.

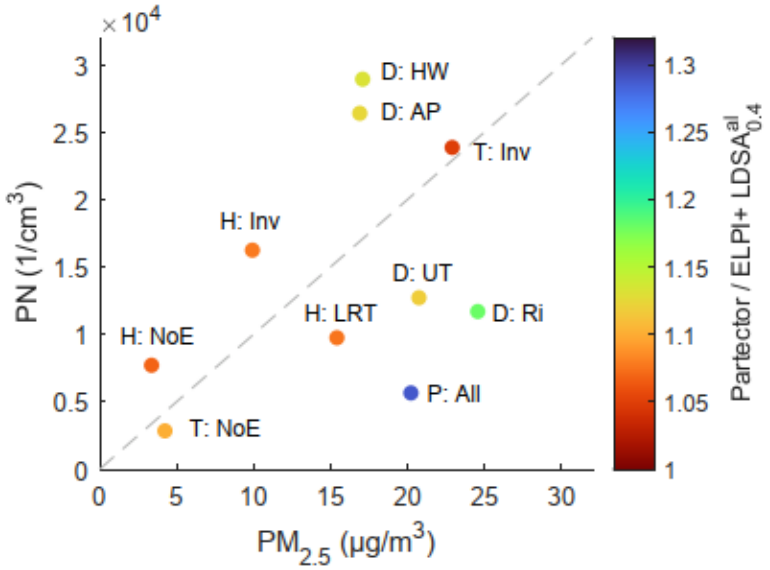

Figure S23: Comparison of $LDSA^{al}$ concentrations measured with Partector and ELPI+ as a function of particle number (PN) and $PM_{2.5}$ concentration. With ELPI+ only particles smaller than 400 nm are considered ($LDSA^{al}_{0.4}$). Each dot represents individual measurements in different locations (Table S2).

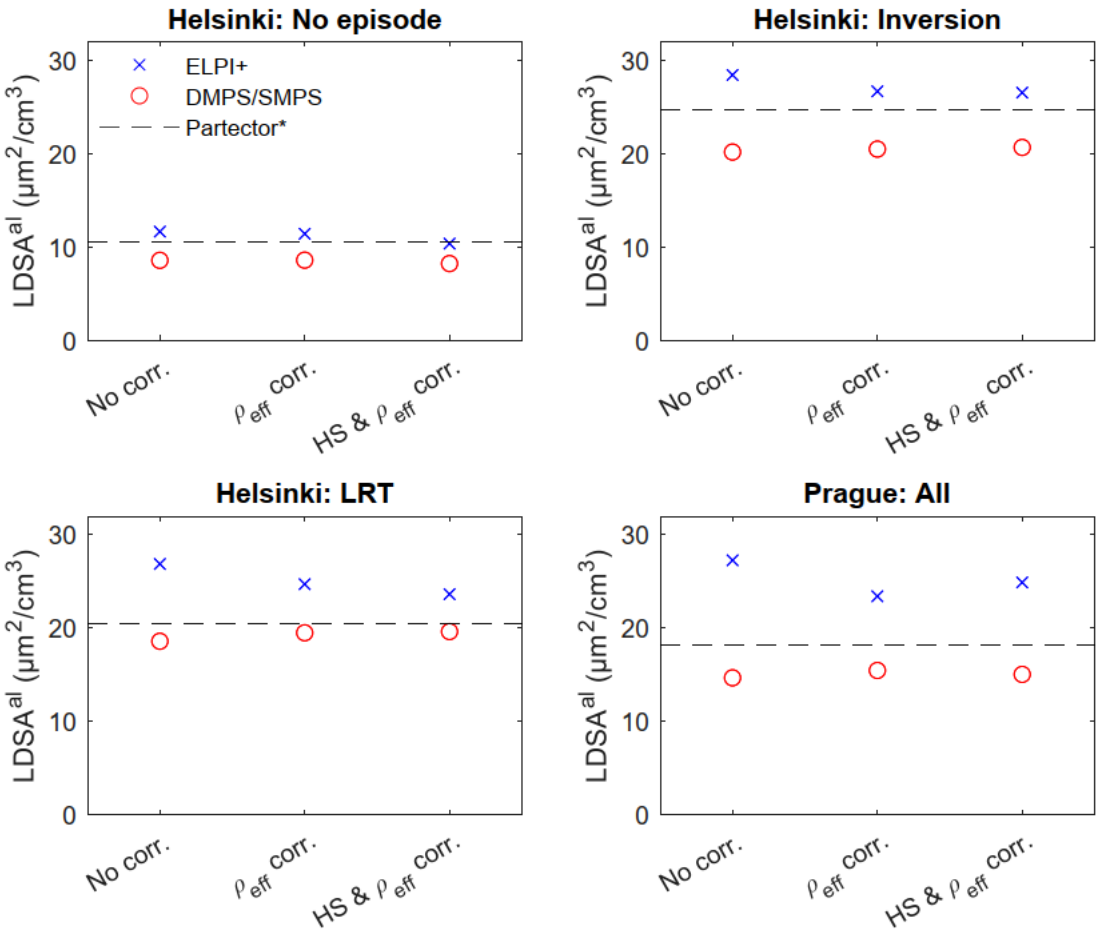

Figure S24: Comparison of average $LDSA^{al}$ concentrations. "No corr." indicates data measured with the general assumptions, "ρ_{eff} corr." indicates data corrected with the effective density and "ρ_{eff} &HS corr." indicates data corrected with both effective density and hygroscopicity. The DMPS measured in Helsinki, and the SMPS in Prague. *Note that the corrections cannot be done with the Partector data.

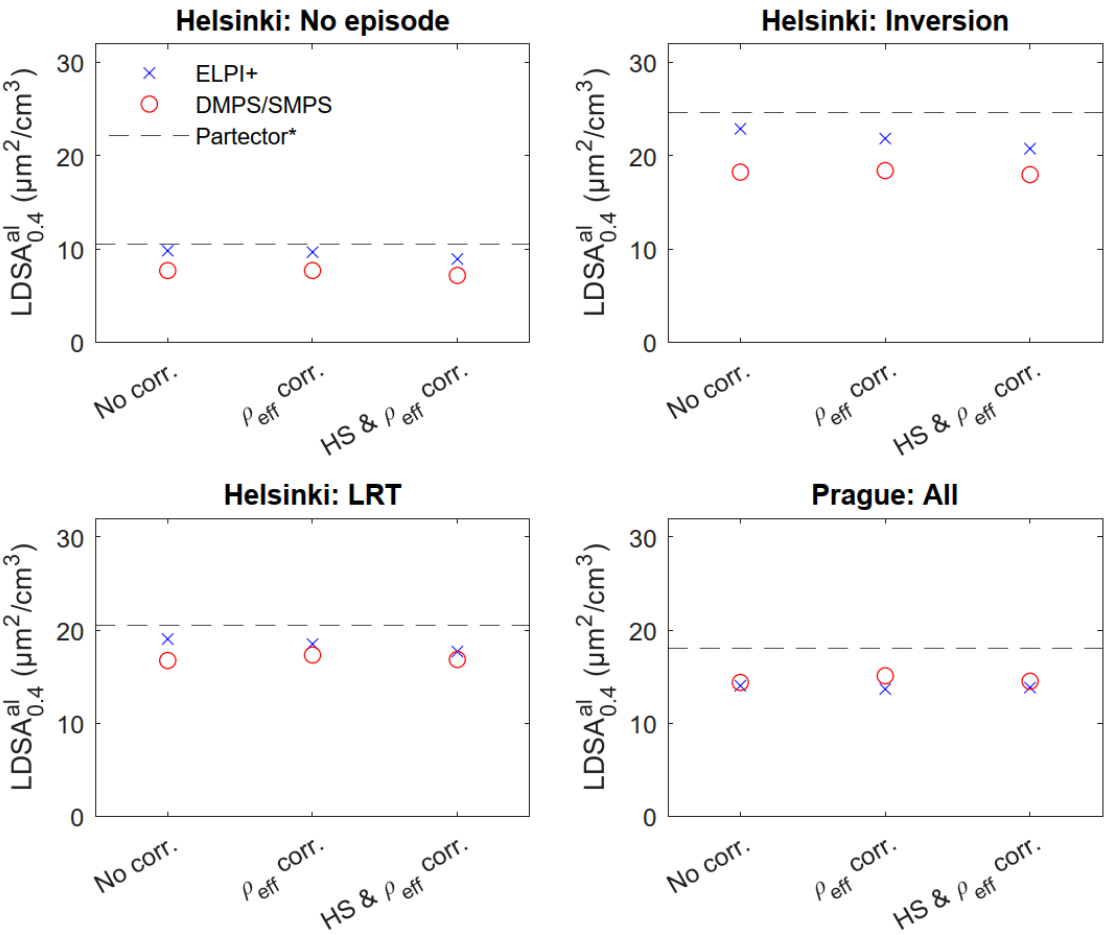

Figure S25: Comparison of average LDSA^{al} concentrations attributable to particles smaller than 400 nm. "No corr." indicates data measured with the general assumptions, "ρ_{eff} corr." indicates data corrected with the effective density and "ρ_{eff} &HS corr." indicates data corrected with both effective density and hygroscopicity. The DMPS measured in Helsinki, and the SMPS in Prague. *Note that the corrections cannot be done with the Partector data.